Tetrahedron Vol. 37, pp. 2341 to 2349, 1981
Printed in Great Britain.

0040-4020/81/132341-09$02.00/0
Pergamon Press Ltd.

POLYBROMINATED OXYDIPHENOL DERIVATIVES FROM THE SPONGE *DYSIDEA HERBACEA*

STRUCTURE DETERMINATION BY ANALYSIS OF ^{13}C SPIN-LATTICE RELAXATION DATA FOR QUATERNARY CARBONS AND ^{13}C–^{1}H COUPLING CONSTANTS

RAYMOND S. NORTON,* KEVIN D. CROFT† and ROBERT J. WELLS*

Roche Research Institute of Marine Pharmacology, P. O. Box 255, Dee Why, 2099, Australia

(*Received in U.S.A. 8 May* 1980)

Abstract—Five polybrominated oxydiphenol derivatives have been isolated from various Great Barrier Reef collections and one Fijian collection of the sponge *Dysidea herbacea*: 3,4,4',5,6,6'-hexabromo-2, 2'-oxydiphenol (**11**), 3,4',5,6,6'-pentabromo-2,2'-oxydiphenol (**12**), 3,4',5,6,6'-pentabromo-2,2'-oxydiphenol 1-methyl ether (**13**), 3,4,4',5,6'-pentabromo-2,2'-oxydiphenol 1,1'-dimethyl ether (**14**) and 3,4',5,6'-tetrabromo-2,2'-oxydiphenol 1'-methyl ether (**15**).

The structure of the first member of this series is determined by a new method involving ^{13}C spin-lattice relaxation data. The contributions of nearby hydrogens to quaternary carbon spin-lattice relaxation times are calculated for various possible structures and compared with the experimental data, leading to an unequivocal proof of structure. The structures of the remaining compounds in the series are established principally by analysis of ^{13}C chemical shifts and ^{13}C–^{1}H coupling constants.

The sponge *Dysidea herbacea* has been the subject of five previous studies[1–5]. A collection of *D. herbacea* from the Caroline Islands in the Pacific Ocean yielded the series of polybrominated diphenyl ethers **1–6**, the structures of which were established by the synthesis of various representatives[1]. More recently, separate collections of *D. herbacea* from the Great Barrier Reef gave the novel tetramic acid derivative dysidin **7**,[2] the hexachloro-metabolites dysidenin **8**,[3] and isodysidenin **9**,[4] and the diketopiperazine **10**.[5] It is evident from these reports that *D. herbacea* is a chemically diverse species, that several distinct species exist which are morphologically indistinguishable, or that different algal or bacterial symbionts associated with the sponge are responsible for the significant variation in major secondary metabolites among different collections of the sponge.

There are two main aspects of the present report. It describes the isolation and structure determination of five polybrominated oxydiphenol derivatives **11–15** from a number of collections of *D. herbacea* from the Great Barrier Reef as well as one Fijian collection. Compounds **11–15** are related to the diphenyl ethers **1–6** isolated previously from *D. herbacea*, but differ in that they are all oxygenated on both phenyl rings instead of only one. As well as this, a method of structure determination is described which employs ^{13}C spin-lattice relaxation data for quaternary carbons. This approach is used to establish the structure of the first member of this series of compounds (**11**), the remaining structures being solved principally by analysis of ^{13}C–^{1}H coupling constants. The isolation of another brominated oxydiphenol derivative (**16**), also from *D. herbacea*, was reported recently by us.[6]

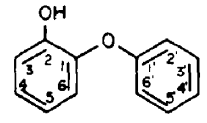

1: 3,4,5,2',4'-pentabromo
2: 4,5,6,2',4'-pentabromo
3: 3,5,2',4'-tetrabromo
4: 4,6,4'-tribromo
5: 3,4'-dibromo
6: 6,4'-dibromo

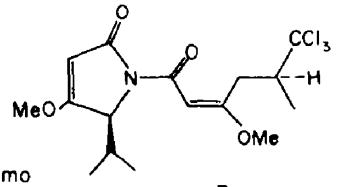

7

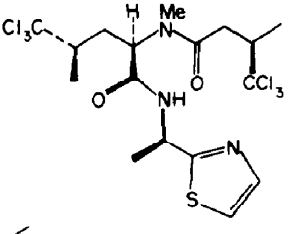

8

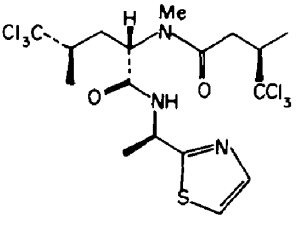

9

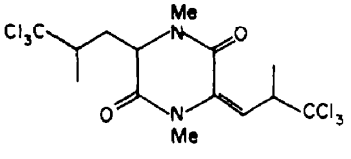

10

†Permanent address: School of Natural Resources, University of the South Pacific, Suva, Fiji.

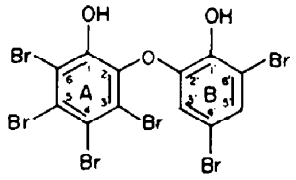

11

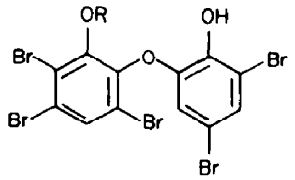

12: R = H
13: R = Me

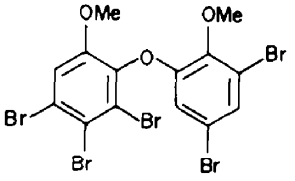

14

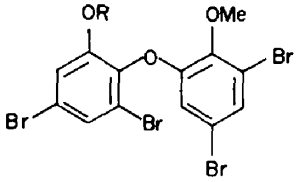

15: R = H
16: R = Me

RESULTS AND DISCUSSION

Brominated oxydiphenol derivatives were obtained from collections of *D. herbacea* made at Lizard Island and Feather Reef on the Great Barrier Reef, at a site near Gladstone, and at Nasese Point, near Suva. Freeze-dried sponge was extracted with dichloromethane, the extract chromatographed on silica gel, and the individual metabolites separated by PLC or HPLC on silica gel.

3,4,4',5,6,6'-*Hexabromo*-2,2'-*oxydiphenol* (**11**). *Structural elucidation using* ^{13}C *spin-lattice relation times.* The molecular formula $C_{12}H_4O_3Br_6$ was established by high resolution mass spectrometry and suggested a structure similar to those previously established for **1–6**. The ^1H NMR spectrum showed resonances due to a pair of *meta*-coupled protons at δ 6.36 and 7.21 (both doublets, $J = 2$ Hz), indicating that one benzene ring is completely substituted.

Table 1 shows the relevant ^{13}C NMR parameters for the parent compound **11** and a derivative **11a** in which the two OH protons have been replaced by deuterium. Comparison of the ^{13}C–^1H spin coupling constants for **11** and **11a** shows that they are not affected by replacement of the OH protons with deuterium. This indicates that the OH protons of both rings are exchanging too rapidly at 33° to participate in measurable ^{13}C–^1H spin–spin coupling. The absence of measurable ^{13}C–^1H coupling for peaks 1,4, 6–8 and 10 (Table 1) requires that they be assigned to carbons of ring A (structure diagram). The resonances of the remaining six carbons (peaks 2, 3, 5, 9, 11 and 12) all exhibit ^{13}C–^1H spin coupling. Peaks 5 and 9 are assigned to the two H-bearing carbons on the basis of their large ^{13}C-^1H coupling constants and short ^{13}C T_1 values (see below). Peaks 1–4 are assigned to O-bearing carbons on the basis of chemical shift,[7] and the remaining quaternary carbon resonances 6–8 and 10–12 are assigned to brominated carbons by elimination, this assignment being confirmed below by ^{13}C T_1 values.

In order to determine the substitution pattern in the B ring it is necessary to differentiate the ether carbon resonance from that of the OH-bearing carbon. The effect of deuterium substitution on ^{13}C–^1H coupling constants is negligible in the present case, and the effect on chemical shifts (Table 1), while it suggests that peak 3 rather than peak 2 be assigned to C–1', is not convincing. However, the effect of deuterium substitution on the ^{13}C spin-lattice relaxation time of the C–1' resonance is quite significant. The following discussion outlines the basis for its interpretation.

Many different relaxation mechanisms can contribute to the relaxation of ^{13}C nuclei,[8,9] but the spin-lattice relaxation of most H-bearing carbons is dominated by ^{13}C–^1H dipole–dipole interactions with directly-bonded hydrogens.[9–11] Relaxation of quaternary carbons is also dominated by ^{13}C–^1H dipolar interactions in many cases,[9–12] at least at low magnetic field strengths where the chemical shift anisotropy relaxation mechanism[8] can be safely ignored.[13,14]

When a molecule is undergoing isotropic rotational reorientation, the contribution of ^{13}C–^1H dipolar interactions to T_1 of a ^{13}C nucleus (under conditions of complete proton decoupling) is given by eqn (1),[8]

$$\frac{1}{T_1} = \sum_K \frac{1}{T_{1K}} = \frac{1}{10}\hbar^2\gamma_C^2\gamma_H^2\chi\sum_K r_{CH_K}^{-6} \qquad (1)$$

where γ_C and γ_H are the gyromagnetic ratios of ^{13}C and ^1H, respectively, r_{CH_K} is the distance from the ^{13}C nucleus to proton K, and χ is given by eqn (2),

$$\chi = \frac{\tau_R}{1+(\omega_H-\omega_C)^2\tau_R^2} + \frac{3\tau_R}{1+\omega_C^2\tau_R^2} + \frac{6\tau_R}{1+(\omega_H+\omega_C)^2\tau_R^2} \qquad (2)$$

τ_R is the correlation time for rotational reorientation of the molecule, and ω_C and ω_H are the resonance frequencies in radians/sec of ^{13}C and ^1H, respectively: Equation (1) was derived for the case in which internal motions are much slower than the overall rotational reorientation of the molecule.[8]

In the case of H-bearing carbons, only interactions with directly-bonded hydrogens have to be considered, and eqn (1) becomes,

$$\frac{1}{T_1} = \frac{N}{10}\hbar^2\gamma_C^2\gamma_H^2\chi r_{CH}^{-6} \qquad (3)$$

where N is the number of directly-bonded hydrogens and r_{CH} the C–H bond length. In the absence of internal motions eqn (3) can be used to obtain τ_R from the

Table 1. ^{13}C Chemical shifts, ^{13}C-^{1}H coupling constants, and ^{13}C spin-lattice relaxation times and integrated intensities for **11**

Peak[a]	Assignment[b]	**11** (-OH)[c]					**11a** (-OO)[d]					T_1^{CH}(OH)[j]
		δ[e]	J_{CH}[f]	n[g]	T_1[h]	T_1^{CH}[i]	δ[e]	J_{CH}[f]	n[g]	T_1[h]	T_1^{CH}[i]	
1	C-1	149.0	n.d.[k]	1.8	4.0	4.0	148.8	n.d.	0.4	8.1	42.4	4.6
2	C-2'	145.6	3.7(d),1.8(d)	2.1	4.5	4.5	145.5	3.7(d),1.8(d)	1.7	7.6	7.6(9.1)[l]	23.4(13.8)
3	C-1'	143.9	7.0(t)	2.1	3.5	3.5	143.7	7.0(t)	0.7	13.4	39.2	4.0
4	C-2	139.5	n.d.	1.7	7.9	7.9(9.4)[l]	139.5	n.d.	0.9	12.1	26.8	13.2(18.0)
5	C-5'	128.4	172.9(d),6.0(d)	2.0	0.11	0.11	128.4	173.3(d),6.1(d)	2.0	0.15	0.15	q
6	m	125.5	n.d.	0.2	6.0	49.8	125.5	n.d.	0.1	8.6	122.2	110
7	m	120.3	n.d.	0.3	6.4	47.2	120.2	n.d.	0.3	8.5	49.8	q
8	m	117.4	n.d.	0.3	6.7	40.4	117.4	n.d.	0.2	9.9	78.8	130
9	C-3'	115.6	166.6(d),6.7(d)	2.5	-[n]	-	115.6	167.2(d),6.7(d)	2.3	0.16[o]	0.16	
10	m	115.6	n.d.		6[o]	25[p]	115.4	n.d.		-[n]	-	
11	C-6'	111.2	3.7(d),1.2(d)	1.4	3.4	4.9	111.1	3.7(d),1.2(d)	1.2	4.5	7.5	45
12	C-4'	109.5	4.9(t)	1.6	2.5	3.2	109.6	4.9(t)	1.6	3.4	4.3	q

[a] Numbered consecutively from downfield end of spectrum. [b] See text. [c] 0.8 M in DMSO-d_6 at 33°C. [d] 0.5 M deuterated sample (see Experimental) in DMSO-d_6 containing 7% (v/v) D_2O. [e] Chemical shift in ppm from TMS. [f] ^{13}C-^{1}H coupling constant in Hz (multiplicity in parentheses). [g] ^{13}C NOE normalised by setting the intensity of peak 5 equal to 2.99. [h] ^{13}C spin-lattice relaxation time (in sec.). [i] Contribution (in sec.) of ^{13}C-^{1}H dipolar interactions to observed T_1, obtained from eqn. (5) as discussed in text. [j] Obtained from eqn. (6) as discussed in text. [k] No ^{13}C-^{1}H spin coupling detected under the spectral accumulation conditions employed. [l] See Experimental. [m] Peaks 6, 7, 8 and 10 are assigned to C-3, C-4, C-5, and C-6, but not on a one-to-one basis. [n] T_1 value not obtained because of peak overlap. [o] Approximate T_1 value (see Experimental). [p] Approximate T_1^{CH} obtained from the observed T_1 value by assuming that n = 0.5 for peak 10. [q] Deuteration has no effect.

measured T_1 values of H-bearing carbons. For **11** in DMSO-d_6 only one of the methine carbon resonances is sufficiently well resolved to permit an accurate T_1 measurement. Therefore it cannot be established that **11** behaves as an isotropic rigid rotor in this solvent. However, both resonances are resolved in **11a** and they have equal T_1 values (Table 1), suggesting that this description is an acceptable approximation. τ_R values of 0.45 and 0.33 nsec are then obtained for **11** and **11a**, respectively, from eqn (3) by setting $r_{CH} = 1.10$ Å.

These τ_R values satisfy the "extreme narrowing" condition

$$(\omega_H + \omega_C)^2 \tau_R^2 \ll 1 \tag{4}$$

Thus, the resonances of H-bearing carbons experience the maximum nuclear Overhauser enhancement (η) of 1.99 in fully proton-decoupled spectra (Experimental). The contribution of ^{13}C–^1H dipolar interactions to T_1 of a quaternary carbon is then given by eqn (5),

$$T_1^{CH} = \frac{1.99}{\eta} T_1^{\text{total}} \tag{5}$$

Experimental values of T_1^{CH} are given in Table 1. These values are valid regardless of whether or not relaxation of the quaternary carbons is dominated by ^{13}C–^1H dipolar interactions. However, T_1^{CH} values obtained for resonances with large nuclear Overhauser enhancements are subject to smaller percentage experimental errors because of the error of about ±0.3 in experimental intensities.

In the case of quaternary carbons the contribution of ^{13}C–^1H dipolar interactions to spin-lattice relaxation is weak because of the dependence of T_1 on the sixth power of the C–H distance (eqn (1)). An important consequence of this sixth power dependence is that the major ^{13}C–^1H dipolar contributions to spin-lattice relaxation times of quaternary carbons come from protons two bonds removed (typical $r_{CH} = 2.15$ Å). For example, a proton three bonds removed and having $r_{CH} = 3.1$ Å contributes 1/9 as much to relaxation as a proton 2.15 Å away. Applying this to the present case, it can be predicted that T_1^{CH} for the two OH-bearing carbons should increase significantly upon deuterium substitution because the number of hydrogens two bonds removed would decrease by one. Indeed, now that τ_R is known, it is possible to calculate this change fairly accurately from eqn (1) because distances from protons that are two bonds removed and attached to oxygen are typically about 2.0 Å[11,15]. Thus, the OH proton should contribute 4.0 sec to T_1^{CH} of the carbons attached to OH groups in **11**.

The effects of deuterium substitution on T_1^{CH} values are readily calculated from eqn (6),

$$[T_1^{CH}(\text{OH})]^{-1} = [T_1^{CH}(\mathbf{11})]^{-1} - [T_1^{CH}(\mathbf{11a}) \times \tfrac{0.33}{0.45}]^{-1} \tag{6}$$

the correction to T_1^{CH} values in **11a** being necessary to account for the difference in τ_R values. The calculated values are given in the last column of Table 1. Two peaks, 1 and 3 have T_1^{CH} (OH) values near 4 sec and are therefore assigned to OH-bearing carbons. This confirms that each ring contains one OH substituent.

The remaining substitution pattern in ring B follows readily from T_1^{CH} values. In **11a**, one proton two bonds removed from a quaternary carbon (typical $r_{CH} = 2.15$ Å) should contribute 8.4 sec to T_1^{CH}. Comparing this with the T_1^{CH} values obtained for **11a** (penultimate column in Table 1), it follows that the OH-bearing carbon (peak 3) has no *ortho* proton in **11a**, the ether carbon (peak 2) and one of the ring B brominated carbons (peak 11) have one each, and the other brominated carbon (peak 12) has two. This is consistent only with the substitution pattern in **11**. However, it should be emphasized that once the assignment of the OH-bearing carbon had been established the substitution pattern in ring B could have been obtained from long-range ^{13}C–^1H coupling constants (discussed below).

It now remains to determine the substituent pattern in ring A. The OH-bearing carbon and ether carbon of this ring give rise to peaks 1 and 4, respectively, the brominated carbons to peaks 6–8 and 10. Data in the last column of Table 1 show that deuteration has an even stronger effect on T_1^{CH} of peak 4 than it does on peak 2 (the ether carbon of ring B). This immediately suggests that the OH group in ring A is *ortho* to the ether carbon as in ring B, as the proton of a *meta* substituted OH would have a negligible effect on T_1^{CH}. However, before drawing this conclusion, it is necessary to establish that the OH proton of ring B cannot approach the ether carbon of ring A closely enough to account for the effect of deuteration on T_1^{CH} of the latter. This is achieved as follows. In **11a**, T_1^{CH} for peak 4 is 26.8 sec (Table 1), which corresponds to one proton 2.6 Å away or two protons 2.9 Å away (eqn (1)). There are only two non-exchangeable hydrogens in the molecule, one of which (C5'–H) must be > 5.5 Å from C–2 in any conformation. Thus, the other proton (C3'–H) must be about 2.6 Å away from C–2. From a Dreiding model it is clear that, in any conformation where this condition is satisfied, the C–1' hydroxyl proton cannot approach C–2 more closely than about 3 Å. Experimentally, the change in T_1^{CH} of peak 4 when going from **11** to **11a** (Table 1) indicates that a OH proton must be about 2.5 Å away from C–2 in the dihydroxy-form. Therefore, the OH group must be *ortho*- to C–2, this C–H distance being about 2.5 Å.

It should be emphasized that weak contributions of ^{13}C–^1H dipolar interactions to overall ^{13}C relaxation, such as those of H–3' to C–2, must be interpreted with considerable care. In the present example the interpretation is unequivocal because **11a** contains only 2 non-exchangeable protons. Furthermore, the use of a deuterated solvent precludes the possibility of effects due to solvent-bound protons. A factor which could in principle affect our conclusions is intermolecular association, which might bring protons from one molecule close to quaternary carbons of another. This possibility is neglected here for two reasons: (i) the available evidence indicates that overall reorientation in solution is approximately isotropic, a situation unlikely to apply for associated species, and (ii) if "stacking" interactions were significant, they could be expected to affect the relaxation of other quaternary carbons in ring A except C–2, which is not the case experimentally (Table 1).

Thus, the structure of **11** has been determined entirely by analysis of ^{13}C spin-lattice relaxation data for quaternary carbons. This has been possible without reference to data on model compounds and without invoking arguments based on analogy with other members of the series (see below). Furthermore, no material was consumed in this analysis.

Finally, two details of the data merit further comment: (i) The four brominated carbons in ring A (peaks 6–8 and 10) all have short T_1 values and low NOE. These effects are due to C–Br scalar and dipolar relaxation.[13,16] The strength of this relaxation mechanism relative to that of ^{13}C–^1H dipolar interactions in the same molecule is, however, less than in bromobenzene,[13,16] where the relaxation time of the brominated carbon was similar to that of the *para*- methine carbon. This must also be true for the brominated carbons of ring B, because ^{13}C–^1H dipolar interactions make a larger contribution to the observed T_1 values for quaternary brominated carbons (peaks 11 and 12) than do C–Br interactions (Table 1), whereas in bromobenzene the relaxation of the brominated carbon was dominated by C–Br interactions.[13,16] However, even in **11**, the contribution of C–Br scalar and dipolar interactions to relaxation of the brominated carbons is strong enough to identify their resonances. (ii) As noted above, T_1^{CH} for C-2 in **11a** indicates that one proton, which must be C3'–H, is about 2.6 Å away. This defines a conformation for **11** in which the two rings are tilted with respect to one another at an angle of about 70° (and in which internal motion, if present, is much slower than the rate of overall molecular reorientation). In this conformation C3'–H is located such that it would be shielded by the aromatic "ring current" of ring A. This may account for the observation that one of the ^1H resoances has an unexpectedly high-field chemical shift (δ 6.36 ppm, see above).

Of the five new compounds described here **11** is the most highly substituted. The structures of the remaining members of this series **12–15** can be solved by analysis of ^{13}C chemical shifts and ^{13}C–^1H coupling constants, the latter being more useful than in **11** because **12–15** have larger numbers of protons.

3,4',5,6,6'-*Pentabromo*-2,2'-*oxydiphenol* (**12**). High resolution mass spectrometry indicates a molecular formula $C_{12}H_5O_3Br_5$, while the ^1H NMR spectrum contains a singlet at δ 7.46 in addition to a pair of *meta*-coupled doublets (J = 2 Hz) at δ 6.47 and 7.27, similar to those observed in the spectrum of **11**. These data strongly suggest a structure similar to **11**, but with one of the bromines in ring A replaced by hydrogen. ^{13}C NMR data (Table 2) confirm this, as there are six resonances having chemical shifts and ^{13}C–^1H coupling constants nearly identical with those of C–1' to C–6' of **11**.

The position of the hydrogen in ring A is determined from long-range ^{13}C–^1H coupling constants. In substituted benzene derivatives,[7,17] *ortho* ($^2J_{CH}$) coupling constants are usually smaller than 2 Hz except for carbons substituted with highly electronegative atoms, in which case they can be as large as 5 Hz in magnitude, *meta* ($^3J_{CH}$) coupling constants are in the range 7–10 Hz, and *para* ($^4J_{CH}$) coupling constants are less than 2 Hz. Thus, the observation of a 9.2 Hz coupling to the peak at 139.0 ppm in **12** indicates that the proton in ring A is *meta* to this carbon. As this peak can be assigned to C–2 by comparison with **11** the proton must be at C–4 or C–6. Long-range coupling to C–1 (peak at 150.5 ppm) is consistent with either *ortho* or *para* proton substitution. However, if the proton were attached to C–6, the brominated carbons would be located *ortho*, *meta* and *para* to this carbon and their long-range couplings would reflect this. In contrast, there are two brominated carbon resonances with J_{CH} = 4–4.3 Hz and one with J_{CH} = 9.8 Hz, consistent only with proton substitution at C–4. This establishes structure **12**.

The structure is confirmed by the magnitude of the ^{13}C–^1H coupling constant for the methine carbon in ring A of **12**. In rings B of **11** and **12** the methine carbons flanked by two brominated carbons (C–5') have $^1J_{CH}$ = 172.9 and 173.0 Hz, respectively, whereas those flanked by one brominated and one oxygenated carbon (C–3') have $^1J_{CH}$ = 166.6 and 166.3 Hz, respectively. The observation of $^1J_{CH}$ = 177.0 Hz for the peak at 126.0 ppm in **12** therefore indicates that it must be flanked by two brominated carbons rather than one.

3,4',5,6,6,6'- *Pentabromo* - 2,2' - *oxydiphenol* 1 - *methyl ether* (**13**). The molecular formula ($C_{13}H_7O_3Br_5$) and ^1H NMR spectrum (a OMe singlet at δ 3.80, in addition to a singlet at δ 7.70 and a pair of *meta*-coupled doublets at δ 6.50 and 7.31) of **13** suggest that it is a methyl ether of **12**.

The ^{13}C NMR spectrum contains a set of six resonances with chemical shifts and J_{CH} values essentially identical with those of C–1' to C–6' of **11** and **12** (Table 2), indicating that ring B is identical in all three metabolites. The OMe group must therefore be located at C–1. The long-range ^{13}C–^1H coupling constants for the other carbons in ring A confirm that the remaining substitution pattern is identical with that in **12**.

3,4,4',5,6'-*Pentabromo*-2,2'-*oxydiphenol* 1,1'-*dimethyl ether* (**14**). The molecular formula ($C_{14}H_9O_3Br_5$) and ^1H NMR spectrum (OMe singlets at δ 3.72 and 3.96, a singlet at δ 7.25, and a pair of *meta*-coupled doublets at δ 6.43 and 7.31) of **14** initially suggest that it is simply a methyl ether derivative of **13**. However, the chemical shift of the aromatic singlet is sufficiently different from that in **13** to cast doubt on this.

The long-range ^{13}C–^1H coupling constants for **14** (Table 2) confirm that ring A contains one proton, while ring B contains two. Indeed, from these data it is straightforward to show that the substitution pattern in ring B is identical to that in **11–13**, except for methylation of the oxygen substituent at C–1'. In ring A the ether carbon resonance at 139.4 ppm is coupled to one *meta* proton as in **12** and **14**, but the long-range couplings to the three brominated carbon resonances (all doublets, J_{CH} = 1.8, 4.9 and 8.5 Hz) suggest that the latter are substituted *para*, *ortho* and *meta*, respectively, which requires a proton substituent at C–6. The one bond ^{13}C–^1H coupling constant for the methine carbon (170.6 Hz) is intermediate between the values for carbons flanked by one and two brominated barbons, but is consistent with proton substitution at C–6.

3,4',5,6'-*Tetrabromo*-2,2'-*oxydiphenol* 1'-*methyl ether* (**15**). The molecular formula ($C_{13}H_8O_3Br_4$) and ^1H NMR spectrum indicate the presence of one OMe substituent (δ 3.96) and two pairs of *meta* coupled doublets (δ 6.53 and 7.30, 7.10 and 7.25, all J = 2Hz).

A set of six resonances in the ^{13}C NMR spectrum having chemical shifts and ^{13}C–^1H coupling constants (Table 2) similar to those of ring B of **14**, indicates that the substituent pattern is the same as in the corresponding rings of **11–13**, except for methylation of the oxygen at C–1', as in **14**. That the Me group is located on ring B is further confirmed by the absence of brominated carbon resonances near 109 and 111 ppm. These are characteristic of C–4' and C–6', respectively, of the unmodified ring B in **11–13** (see Table 2).

The substitution pattern in ring A is solved by analysis of ^{13}C–^1H coupling constants. The ether carbon resonance at 137.7 ppm, which is assigned by its chemical shift, is coupled to two meta-substituted protons. The one-bond coupling constants for the methine carbon

Table 2. ^{13}C Chemical shifts and ^{13}C–^{1}H spin–spin coupling constants for **11–16**[a]

Carbon Number[b]	11 δ[c]	11 J_{CH}[d]	12 δ	12 J_{CH}	13 δ	13 J_{CH}	14 δ	14 J_{CH}	15 δ	15 J_{CH}	16 δ	16 J_{CH}
1	149.0	n.d.	150.5	d 1.2	151.8	qa 2	152.0	qi 4	151.8	d 2.9, d 1.4	153.1	m
2	139.5	n.d.	139.0	d 9.2	144.4	d 9.5	139.4	d 8.6	137.7	t 7.6	138.2	t 7.8
3	125.5	n.d.	116.2[f]	d 4.3	117.1[f]	d 4.3	121.5	d 1.8	118.0	d 3.7, d 1.2	117.7	d 3.4, d 1.5
4	120.3	n.d.	126.0	d 177.0	131.9	d 176.9	118.1	d 8.5	125.2	d 175.8, d 6.4	126.5	d 175.8, d 6.1
5	117.4	n.d.	122.2[f]	d 4.0	122.2[f]	d 4.3	122.4	d 4.9	118.9	t 4.0	119.4	t 4.7
6	115.6	n.d.	114.5	d 9.8	121.0	d 9-10	117.9	d 170.6	119.7	d 167.7, d 6.0	116.0	d 166.9, d 5.5
1'	143.9	t 7.0	144.2	t 7.0	143.5	t 7.2	144.9	m	145.0	m	144.8	m
2'	145.6	d 3.7, d 1.8	146.1	d 3.7, d 1.8	145.9	d 3.7, d 1.5	150.8	d 3.7, d 1.8	151.1	d 3.5, d 1.4	150.9	d 3.7, d 1.2
3'	115.6	d 166.6, d 6.7	115.9	d 166.3, d 7.0	116.0	d 167.1, d 6.5	116.3	d 169.7, d 5.8	116.2	d 166.6, d 6.4	116.4	d 168.5, d 6.1
4'	109.5	t 4.9	109.1	t 4.6	109.7	t 4.7	116.3	t 4.6	116.0	t 4.6	116.0	t 4.6
5'	128.4	d 172.9, d 6.0	128.3	d 173.0, d 6.7	128.6	d 173.1, d 6.2	128.5	d 175.2, d 6.1	128.0	d 174.8, d 6.4	128.1	d 175.2, d 5.5
6'	111.2	d 3.7, d 1.2	111.2	d 3.7, d 1.2	111.5	d 3.5, d 1	118.7	d 3.8, d 1.4	118.5	d 3.7, d 1.2	118.5	d 3.7, d 1.2
1-OMe					61.4	qa 147.1	57.1	qa 146.5			56.8	qa 146.5
1'-OMe							60.7	qa 145.9	60.5	qa 145.7	60.4	qa 145.3

[a] In DMSO-d_6. [b] See structure diagram. Assignments follow from ^{13}C chemical shifts and ^{13}C-^{1}H coupling constants. [c] Chemical shifts in ppm from TMS; estimated accuracy 0.1 ppm. [d] ^{13}C-^{1}H coupling constants in Hz; estimated accuracy 1 Hz. d = doublet, t = triplet, qa = quartet, qi = quintet, m = multiplet. [e] ^{13}C-^{1}H coupling not detectable. [f] Assignments may be reversed within the same column.

resonances and the long-range couplings to the brominated carbons can then be satisfied only by placing the Br substituents at C-3 and C-5, thus establishing structure **15**.

3,4',5,6'-Tetrabromo-2,2'-oxydiphenol 1,1'-dimethyl ether (**16**). The structure of this metabolite was solved independently by analysis of ^{13}C spin-lattice relaxation data and ^{13}C–^{1}H coupling constants[6] without reference to the above series of compounds. However, the ^{13}C NMR data in Table 2 show that its structure could have been solved by analogy with those of **11–15**.

The brominated oxydiphenol derivatives described in this paper are all oxygenated on both phenyl rings. The compounds isolated by Sharma and Vig[1] from *D. herbacea* collected in the Caroline Islands are oxygenated on only one phenyl ring. In the accompanying paper,[18] Faulkner *et al.* report the isolation of a number of brominated oxydiphenols (including **11,12** and **16**) from *Phyllospongia foliascens.*

CONCLUDING REMARKS

The structures of **11–16** have been determined using a combination of ^{13}C chemical shifts, ^{13}C–^{1}H coupling constants and ^{13}C spin-lattice relaxation data. The use of relaxation data in this way represents a novel approach in this field. Previously we have shown that the tautomeric form of 1-methylisoguanosine in solution could be defined by quantitative analysis of the contributions of exchangeable protons two bonds removed from the four quaternary carbons in the purine ring to spin-lattice relaxation of the latter.[19] The application of such techniques to determination of the structures of **11** and **16**[6] represents an extension of this approach, and provides an opportunity to evaluate it.

The major drawback of any technique which employs ^{13}C spin-lattice relaxation measurements on quaternary carbons is that such measurements are time-consuming. However, this is to be balanced against the need to record spectroscopic data on model compounds or other natural products related to the compound of interest, to carry out chemical modifications on the parent compound, or to attempt to obtain crystals suitable for X-ray crystallographic analysis, all of which are often necessary using conventional approaches to the solution of unknown structures. It should also be noted that the accumulation and processing of spin-lattice relaxation data is automated on modern spectrometers, whilst data interpretation is straightforward and not dependent on the availability of data for model compounds.

The method is not applicable to all problems. It is most useful in fairly rigid systems, such as those encountered here, in which carbon–hydrogen distances can be estimated with some certainty. We have applied this method successfully to a number of marine natural products[20] in combination with analysis of ^{13}C–^{1}H coupling constants.

The optimal magnetic field strength for the determination of ^{13}C–^{1}H dipolar contributions to spin-lattice relaxation times of quaternary carbons has not been determined. At high magnetic field strengths the chemical shift anisotropy relaxation mechanism becomes significant.[13,14] While this in no way prevents the determination of T_1^{CH} values, it requires that more accurate NOE values be obtained in order to maintain an acceptable accuracy in calculated T_1^{CH} values. The higher sensitivity of high field NMR spectrometers and shorter experimental T_1 values at high field may ensure that the necessary accuracy is maintained without increasing the spectral accumulation time. Nevertheless, it is worth noting that spin-lattice relaxation measurements on spectrometers operating at low to intermediate magnetic field strengths represent a potentially valuable application of such instruments, for which access time is likely to become increasingly available during the next few years as more high field instruments come into service.

EXPERIMENTAL

Materials. All solvents used were of analytical grade. All high performance liquid chromatography (HPLC) was carried out on a Whatman Magnum 9 10/50 partisil semi-preparative column. Plc and tlc separations were performed on Merck Si60 silica gel plates. Deuterated solvents (>99 atom % D) were obtained from Merck, Sharp and Dohme, Montreal.

Isolation of brominated oxydiphenol derivatives from Dysidea herbacea. Freeze dried *D. herbacea* (500 g., RRIMP Museum specimen number FN 1775), collected on Feather Reef, east of Innisfail, Queensland, Australia, was milled and slowly percolated with dichloromethane (5 l) followed by methanol (5 l) to give, after evaporation *in vacuo*, extracts of 12 g and 13 g, respectively. The CH_2Cl_2 extract was triturated with $CHCl_3$ (150 ml), the mixture filtered and the solids washed with $CHCl_3$ to give a pale green powder (4 g) which was shown by tlc to be a 9:1 mixture of **11** and the pentabromo-metabolite **12** (silica gel run in CH_2Cl_2:EtOAc, 3:1). Two recrystallisations from acetonitrile gave pure **11** (2.6 g).

Further supplies of **11** (0.5 g) were isolated from the mother liquors derived from the acetonitrile crystallisation by plc on silica gel (CH_2Cl_2:EtOAc, 4:1). A further 1.5 g was obtained from the MeOH extract by chromatography on Sephadex LH 20 in MeOH to give a mixture of **11** and **12** (2.5 g) which was processed as above.

The $CHCl_3$ soluble material remaining from the isolation of crude **11** was preadsorbed on silica gel (Merck Kieselgel H, 40 g), the solvent removed under vacuum and the remaining powder added to the top of a short column of silica gel (Kieselgel H, 200 g) dry packed into a Buchner funnel under vacuum. This column was developed by application of vacuum with CH_2Cl_2–hexane (1:1, 500 ml), CH_2Cl_2 (700 ml) and EtOAc-MeOH (1 l).

Evaporation of the CH_2Cl_2–hexane fraction gave an oil (700 mg) which was separated by plc to yield **16** (200 mg) and a tribromo-dimethyl ether (10 mg) which was not characterised further.

The material eluted with CH_2Cl_2 (1.10 g) was separated by plc to yield **15** (200 mg) and **13** (30 mg) together with fats and sterols which were not investigated further.

Extraction of 75 gm freeze-dried *D. herbacea* collected at Farmer's Point, near Gladsone, Queensland (RRIMP museum specimen number FN 1864) with CH_2Cl_2 gave an extract containing a single brominated oxydiphenol. Separation on plc afforded 70 mg of **15** as a wax.

A further sample of *D. herbacea* collected near Nasese Point, Suva, Fiji (50 g dry weight, specimen A/16-11-78 held by K. D. Croft) was extracted with CH_2Cl_2 to give 4.5 g of extract. Separation by silica gel chromatography and plc, as above, gave **11** (1.2 g), **12** (0.3 g), **13** (41 mg) and **16** (20 mg) together with mixed fractions containing **14** and **16**, which were separated by preparative hplc using EtOAc–hexane (1:10) with injection volumes of 400 μl of a 10% soln. Quantitative separation was realised to yield 320 mg of **16** and 170 mg of **14**.

3,4,4',5,6,6'-Hexabromo-2,2'-oxydiphenol (**11**) recrystallized from acetonitrile as colourless prisms m.p. 194–195°. (Found: C 21.2; H, 0.8; Br, 70.7%: $C_{12}H_4O_3Br_6$ requires: C, 21.3; H, 0.6; Br, 71.0%). ^{1}H NMR(CD_3OD): δ6.36 (1H, d, J = 2 Hz), 7.21 (1H, d, J = 2 HZ). IR spectrum (nujol): ν_{max} 1580 (b), 1480, 1425, 1405, 1265, 1220, 1205, 950, 930, 840, 770, 690 cm^{-1}. UV spectrum (MeOH): λ_{max} sh 290 (ϵ 5500), 297 (ϵ 6200) nm; (MeOH/NaOH): λ_{max} 315 nm. High resolution mass measurements: Found: 671.5221, $C_{12}H_4O_3{}^{79}Br_5{}^{81}Br_1$ requires: 671.5235; Found: 673.5230, $C_{12}H_4O_3{}^{79}Br_4{}^{81}Br_2$ requires: 673.5216; Found: 675.5172, $C_{12}H_4O_3{}^{79}Br_3{}^{81}Br_3$ requires: 675.5195.

3,4',5,6,6'-Pentabromo - 2,2' - oxydiphenol (**12**) separated from $CHCl_3$ to give colourless crystals, m.p. 183–184°. ^1H NMR spectrum (CD_3OD): δ 6.47 (1H, d, $J = 2$ Hz), 7.27 (1H, d, $J = 2$ Hz), 7.46 (1H, s). IR spectrum (Nujol): ν_{max} 1590, 1575, 1545, 1480, 1235, 1205, 995, 940, 925, 840, 760, 705 cm^{-1}. UV spectrum (MeOH): λ_{max} sh 289 (ϵ 4500), 298 (ϵ 5600) nm; (MeOH/NaOH) λ_{max} 314 nm. High resolution mass measurements: Found: 595.6120, $C_{12}H_5O_3{}^{79}Br_3{}^{81}Br_2$ requires: 595.6110; Found: 597.6100, $C_{12}H_5O_3{}^{79}Br_2{}^{81}Br_3$ requires: 597.6091.

3,4',5,6,6'-Pentabromo-2,2'-oxydiphenol 1-methyl ether (**13**) was recrystallised from $CHCl_3$ to give colourless crystals, m.p. 202–204°. ^1H NMR spectrum (CD_3OD): δ 3.80 (3H, s), 6.50 (1H, d, $J = 2$ Hz), 7.31 (1H, d, $J = 2$ Hz), 7.70 (1H, s). Mass measurement, found *m/e* 606, 608, 610, 612, 614, 616, $C_{13}H_7O_3Br_5$ requires 606, 608, 610, 612, 614, 616.

3,4,4',5,6'-Pentabromo-2,2'-oxydiphenol 1,1'-dimethyl ether (**14**) separated from $CHCl_3$ to give colourless crystals, m.p. 142–144°. ^1H NMR spectrum ($CDCl_3$): δ 3.72 (3H, s), 3.96 (3H, s), 6.43 (1H, d, $J = 2$ Hz), 7.25 (1H, s), 7.31 (1H, d, $J = 2$ Hz). IR spectrum (Nujol): ν_{max} 1565, 1430, 1395, 1350, 1285, 1260, 1245, 1220, 1200, 1180, 1035, 1000, 935, 885, 835, 825, 760 cm^{-1}. UV spectrum (MeOH): λ_{max} sh 282 (ϵ 3200), 290 (ϵ 4000), 299 (ϵ 3000) nm. High resolution mass measurements: Found: 623.6432, $C_{14}H_9O_3{}^{79}Br_3{}^{81}Br_2$ requires: 623.6424; Found: 625.6422, $C_{14}H_9O_3{}^{79}Br_2{}^{81}Br_3$ requires: 625.6403.

3,4',5,6'-Tetrabromo-2,2'-oxydiphenol 1'-methyl ether (**15**) was obtained as a pale green wax, m.p. 32–33°. ^1H NMR spectrum (CD_3OD): δ 3.96 (3H, s), 6.53 (1H, d, $J = 2$ Hz), 7.10 (1H, d, $J = 2$ Hz), 7.25 (1H, d, $J = 2$ Hz), 7.30 (1H, d, $J = 2$ Hz). IR spectrum (Neat): ν_{max} 1580, 1490, 1470, 1430, 1410, 1390, 1285, 1260, 1220, 1020, 1000, 930, 920, 840, 760, 700, 680 cm^{-1}. UV spectrum (MeOH): ν_{max} sh 284 (ϵ 3800), 291 (ϵ 4100) nm; (MeOH/NaOH) λ_{max} 291, 307 nm. High resolution mass measurements: Found: 529.7188, $C_{13}H_8O_3{}^{79}Br_3{}^{81}Br_1$ requires: 529.7182; Found: 531.7160, $C_{13}H_8O_3{}^{79}Br_2{}^{81}Br_2$ requires: 531.7163; Found: 533.7148, $C_{13}H_8O_3{}^{79}Br_1{}^{81}Br_3$ requires: 533.7142.

3,4',5,6'-Tetrabromo-2,2'-oxydiphenol 1,1'-dimethyl ether (**16**) was obtained as an oil[6]. ^1H NMR spectrum ($CDCl_3$): δ3.80 (3H, s), 3.93 (3H, s), 6.42 (1H, d, $J = 2$ Hz), 7.07 (1H, d, $J = 2$ Hz), 7.34 (1H, d, $J = 2$ Hz), 7.44 (1H, d, $J = 2$ Hz). High resolution mass measurements: Found: 543.7332, $C_{14}H_{10}O_3{}^{79}Br_3{}^{81}Br_1$ requires: 543.7340; Found: 545.7313, $C_{14}H_{10}O_3{}^{79}Br_2{}^{81}Br_2$ requires: 545.7320; Found: 547.7294, $C_{14}H_{10}O_3{}^{79}Br_1{}^{81}Br_3$ requires: 547.7299.

Methods. UV spectra were measured on a Hitachi EPS-3T recording spectrophotometer, IR spectra on a Hitachi 285 spectrophotometer, and mass spectra on a VG Micromass 70/70 F system. ^1H NMR spectra were measured in the continuous wave mode on a Jeol MH-100 spectrometer operating at 100 MHz.

^{13}C NMR spectra were obtained at 15.04 MHz on a Jeol FX-60 spectrometer incorporating a 4000-Hz bandpass crystal filter (Jeol), and operating in the pulsed Fourier transform mode. On-resonance, noise-modulated proton decoupling was used unless otherwise indicated and 10 mm o.d. spinning sample tubes were used. Probe temp was 26–30°, except for the T_1 and NOE measurements on **11** which were made at 33°. The sweep width was 2500 Hz in all cases. Spectra were accumulated in 8192 time-domain addresses (giving a digital resolution of 0.61 Hz after Fourier tranformation), except for T_1 measurements on the H-bearing carbons of **11**, where 4096 time-domain addresses were used. Spectra were processed with 1.0 Hz exponential broadening. Chemical shifts were measured digitally and are reported in ppm downfield from internal TMS. The solvent CD_3 resonance at 39.5 ppm was employed as primary standard. Estimated accuracy is 0.1 ppm. ^{13}C–^1H spin–spin coupling constants were measured from spectra recorded with proton irradiation gated off during data acquisition, and on during the remainder of the cycle.

Spin-lattice relaxation times were determined by the inversion-recovery method,[23] in which a $(180°\text{-}\tau\text{-}90°\text{-}t)_n$ pulse sequence was employed. The delay time, t, between each 90° radiofrequency pulse and the following 180° radiofrequency pulse was greater than 5 times the longest T_1 being measured in all cases. The width of a 90° pulse was 17 μsec. T_1 values were determined from the least squares slopes of plots of $\ln(M_0 - M_\tau)$ versus τ where M_0 is the thermal equilibrium value of the magnetisation and M_τ is the initial value of the magnetisation following a 90° pulse at time τ. Only values of $\tau \leq T_1$ were employed in calculating final T_1 values. Separate sets of inversion-recovery sequences were used for measuring H-bearing and quaternary carbon T_1 values in each case. The T_1 of peak 10 of compound **11** was estimated by subtracting the height of the fully-relaxed H-bearing carbon component from the measured height at each τ value. A slight chemical shift difference between the two components in **11a** prevented application of this procedure. The relaxation of the brominated quaternary carbons was observably nonexponential,[13,16] but no attempt was made to analyse the data to obtain more than one relaxation time. Estimated accuracy of T_1 values is 10%.

Integrated intensities were obtained digitally from fully-relaxed spectra recorded with 90° radiofrequency pulse excitation. Resonances of H-bearing carbons were shown to have the full NOE by comparing intensities in spectra recorded with complete proton decoupling with those in spectra recorded with proton decoupling gated on only during data acquisition.[22] The experimental intensities reported in Table 1 (fully decoupled spectra) were adjusted to give a value of 2.99 to the intensity of peak 5. The intensity of peak 10 in each case was estimated by assuming that the methine carbon peak 9 had an intensity of 2.99. Estimated accuracy of integrated intensities is ±0.3. In the case of peak 4 of compound **11** and peak 2 of **11a** the normalised integrated intensities were 2.7 (Table 1), and two T_1^{CH} values were calculated from eqn (5) by assuming tht 2.7 represented the full NOE or a real deviation from the full NOE in each case (Table 1).

Compound **11** was deuterated by incubating in DMSO-d_6 containing 10% D_2O for 30 min at 30°, then adding excess D_2O and lyophilising. The dried sample was dissolved in DMSO-d_6 containing 7% D_2O for the ^{13}C NMR measurements.

Acknowledgements—We thank the marine biology staff of this Institute for Australian collections, Prof. P. Bergquist and Dr. I. G. Skinner for sponge identification, and R. Lidgard for mass spectrometry. R. S. Norton thanks the Queen's Fellowships Committee for the award of a Fellowship in Marine Science during the initial stage of this work, and K. D. Croft thanks the Institute of Marine Resources, University of the South Pacific, for financial assistance.

REFERENCES

[1]G. M. Sharma, B. Vig and P. R. Burkholder, *Food-Drugs from the sea, Proc.* Marine Technol. Soc. 307 (1969); G. M. Sharma and B. Vig, *Tetrahedron Lett.* 1715 (1972).
[2]W. Hofheinz and W. E. Oberhänsli, *Helv. Chim. Acta* **60**, 660 (1977).
[3]R. Kazlauskas, R. O. Lidgard, R. J. Wells and W. Vetter, *Tetrahedron Lett.* 3183 (1977).
[4]C. Charles, J. C. Braekman, D. Daloze, B. Tursch and R. Karlsson, *Ibid* 1519 (1978).
[5]R. Kazlauskas, P. T. Murphy and R. J. Wells, *Ibid* 4945 (1978).
[6]R. S. Norton and R. J. Wells, *Ibid* 3801 (1980).
[7]J. B. Stothers, *Carbon-13 NMR Spectroscopy.* Academic Press, New York (1972); F. W. Wehrli and T. Wirthlin, *Interpretation of Carbon-13 NMR Spectra.* Heyden London (1976).
[8]A. Abragam, *The Principles of Nuclear Magnetism.* Oxford University Press, London (1961); T. C. Farrar and E. D. Becker, *Pulse and Fourier Transform NMR.* Academic Press, New York (1971).
[9]F. W. Wehrli, *Topics in Carbon-13 NMR Spectroscopy* **2**, 343 (1976).
[10]A. Allerhand, D. Doddrell and R. Komoroski, *J. Chem. Phys.* **55**, 189 (1971).
[11]E. Oldfield, R. S. Norton and A. Allerhand, *J. Biol. Chem.* **250**, 6368; 6381 (1975).
[12]R. S. Norton and R. Kazlauskas, *Experientia* **36**, 276 (1980).
[13]G. C. Levy, J. D. Cargioli and F. A. L. Anet, *J. Am. Chem. Soc.* **95**, 1527 (1973).

[14]G. C. Levy and U. Edlund, *Ibid.* **97**, 5031 (1975); R. S. Norton, A. O. Clouse, R. Addleman and A. Allerhand, *Ibid.* **99**, 79 (1977).
[15]*Tables of Interatomic Distances and Configuration in Molecules and Ions*. Chem. Soc. Spec. Publ. No. 11, Suppl. No. 18, (1965).
[16]R. S. Norton, *Tetrahedron* **33**, 2577 (1977); R. S. Norton, R. G. Warren and R. J. Wells, *Tetrahedron Lett.* 3905 (1977).
[17]H. E. Gottlieb, *Isr. J. Chem.* **16**, 57 (1977).
[18]B. Carté and D. J. Faulkner, *Tetrahedron* **37**, 2335 (1981).
[19]R. S. Norton, R. P. Gregson and R. J. Quinn, *J. Chem. Soc. Chem. Commun.* 339 (1980).
[20]R. S. Norton and R. J. Wells, Submitted for publication.
[21]G. C. Levy and I. R. Peat, *J. Magn. Reson.* **18**, 500 (1975).
[22]R. Freeman, H. D. W. Hill and R. Kaptein, *Ibid.* **7**, 327 (1972); S. J. Opella, D. J. Nelson and O. Jardetzky, *J. Chem. Phys.* **64**, 2533 (1976).